

## RESEARCH ARTICLE

10.1002/2016WR019641

### Key Points:

- GRACE TWS and SMOS SM observations were jointly assimilated for the first time
- Joint assimilation improved water balance component estimates, especially in SM profile and groundwater
- Joint assimilation performs better than assimilation of GRACE or SMOS only

### Supporting Information:

- Supporting Information S1

### Correspondence to:

S. Tian,  
siyuan.tian@anu.edu.au

### Citation:

Tian, S., P. Tregoning, L. J. Renzullo, A. I. J. M. van Dijk, J. P. Walker, V. R. N. Pauwels, and S. Allgeyer (2017), Improved water balance component estimates through joint assimilation of GRACE water storage and SMOS soil moisture retrievals, *Water Resour. Res.*, 53, 1820–1840, doi:10.1002/2016WR019641.

Received 12 AUG 2016

Accepted 23 JAN 2017

Accepted article online 31 JAN 2017

Published online 3 MAR 2017

# Improved water balance component estimates through joint assimilation of GRACE water storage and SMOS soil moisture retrievals

Siyuan Tian<sup>1</sup> , Paul Tregoning<sup>1</sup> , Luigi J. Renzullo<sup>2</sup>, Albert I. J. M. van Dijk<sup>3</sup> , Jeffrey P. Walker<sup>4</sup> , Valentijn R. N. Pauwels<sup>4</sup> , and Sébastien Allgeyer<sup>1</sup> 

<sup>1</sup>Research School of Earth Sciences, Australian National University, Canberra, Australian Capital Territory, Australia, <sup>2</sup>CSIRO Land and Water, Canberra, Australian Capital Territory, Australia, <sup>3</sup>Fenner School of Environment and Society, Australian National University, Canberra, Australian Capital Territory, Australia, <sup>4</sup>Department of Civil Engineering, Monash University, Clayton, Victoria, Australia

**Abstract** The accuracy of global water balance estimates is limited by the lack of observations at large scale and the uncertainties of model simulations. Global retrievals of terrestrial water storage (TWS) change and soil moisture (SM) from satellites provide an opportunity to improve model estimates through data assimilation. However, combining these two data sets is challenging due to the disparity in temporal and spatial resolution at both vertical and horizontal scale. For the first time, TWS observations from the Gravity Recovery and Climate Experiment (GRACE) and near-surface SM observations from the Soil Moisture and Ocean Salinity (SMOS) were jointly assimilated into a water balance model using the Ensemble Kalman Smoother from January 2010 to December 2013 for the Australian continent. The performance of joint assimilation was assessed against open-loop model simulations and the assimilation of either GRACE TWS anomalies or SMOS SM alone. The SMOS-only assimilation improved SM estimates but reduced the accuracy of groundwater and TWS estimates. The GRACE-only assimilation improved groundwater estimates but did not always produce accurate estimates of SM. The joint assimilation typically led to more accurate water storage profile estimates with improved surface SM, root-zone SM, and groundwater estimates against in situ observations. The assimilation successfully downscaled GRACE-derived integrated water storage horizontally and vertically into individual water stores at the same spatial scale as the model and SMOS, and partitioned monthly averaged TWS into daily estimates. These results demonstrate that satellite TWS and SM measurements can be jointly assimilated to produce improved water balance component estimates.

## 1. Introduction

The ability to accurately estimate terrestrial water storage (TWS) and its components (e.g., soil moisture, groundwater, surface water, snow, and ice) is critical for hydrological studies and water resource assessment and management. Constraining water balance estimates with satellite observations over large areas offers better potential for assessing water availability, especially in areas with sparse ground observations. Data assimilation is an effective approach to optimally combine information from both model predictions and observations. Measurements of water cycle components have been integrated into hydrological models in a number of studies, including measurements of precipitation [e.g., Joyce *et al.*, 2004; Huffman *et al.*, 2007], soil moisture [e.g., Walker and Houser, 2001; Reichle and Koster, 2005; Draper *et al.*, 2009; Renzullo *et al.*, 2014; Dumedah *et al.*, 2015], TWS [e.g., Zaitchik *et al.*, 2008; Li *et al.*, 2012; van Dijk *et al.*, 2014; Eicker *et al.*, 2014; Tangdamrongsub *et al.*, 2015], and snow [e.g., Sun *et al.*, 2004; Rodell and Houser, 2004; Andreadis and Lettenmaier, 2006]. In many cases, assimilation improved the model estimates.

As a key component in the water cycle, soil moisture (SM) controls the water and energy exchange between the atmosphere and land surface. However, the estimation of soil moisture distribution within the profile at large scales remains challenging due to the lack of root-zone SM observations. The assimilation of near-surface SM observations has been shown to improve near-surface as well as root-zone soil water balance

estimates and, in some cases, also produced improved estimates of evaporation, runoff, or deep drainage [Walker *et al.*, 2001; Reichle and Koster, 2005; Brocca *et al.*, 2010; Renzullo *et al.*, 2014; Draper *et al.*, 2011]. A number of recent studies [Dumedah *et al.*, 2015; Lievens *et al.*, 2015; Martens *et al.*, 2015] assimilated SM retrievals from the SMOS (Soil Moisture and Ocean Salinity) satellite mission [Kerr *et al.*, 2001] into land surface models. SMOS is the first polar-orbiting, space-born, 2-D interferometric L-band radiometer, fully dedicated to the retrieval of surface SM and ocean salinity. Martens *et al.* [2015] found that SMOS SM retrievals sourced from the Level 3 CATDS (Centre Aval de Traitement des Données SMOS) product [Jacquette *et al.*, 2010] have high quality over Australia. The same SMOS SM retrievals were used in this study. Since SM moisture profile estimates can be improved by the assimilation of surface SM observations, it might be expected that total water storage estimated will also be improved. However, so far this hypothesis has not been tested.

The absence of integrated TWS measurements as an overall water balance constraint was resolved with the launch of the GRACE (Gravity Recovery and Climate Experiment) mission in 2002. It provides a complement to traditional ground-based hydrological measurements which are restricted to the scales of sites or individual catchments. The observed mass changes are the combined result of changes in surface water, soil water, groundwater, vegetation water, snow, and ice [Tapley *et al.*, 2004]. Therefore, ancillary data sets or model-based methods are needed to partition GRACE-observed mass change into changes in the individual water components.

GRACE-observed TWS is most commonly provided as an integrated monthly averaged water storage change, known as the TWS anomaly (TWSA). An issue that requires much consideration is how to down-scale, in a temporal sense, the monthly GRACE TWSA estimates to the high temporal frequency of the hydrologic model. Zaitchik *et al.* [2008] assimilated monthly GRACE TWS estimates into the Catchment Land Surface Model (CLSM) using an ensemble Kalman smoother (EnKS)-like approach and distributed the increments evenly over each day of the month. Li *et al.* [2012] and Forman *et al.* [2012] applied a similar method as in Zaitchik *et al.* [2008] and showed the benefits of assimilation in drought monitoring and snow water equivalent estimation. Furthermore, the drought indicators based on assimilated GRACE data, in particular the groundwater storage drought indicator, showed their great value for drought detection [Houborg *et al.*, 2012]. Eicker *et al.* [2014] and Schumacher *et al.* [2016] assimilated GRACE data using an ensemble Kalman filter (EnKF) to jointly update model states and parameters at monthly time steps with consideration of spatial covariance. Tangdamrongsub *et al.* [2015] also implemented an EnKF to assimilate GRACE data into a model considering hydrological routing and demonstrated that GRACE data assimilation can improve overall model behavior but with little improvement in streamflow estimates. van Dijk *et al.* [2014] developed an "off-line" assimilation scheme combining GRACE, satellite water level data, and hydrological models for global water cycle reanalysis. All these studies demonstrate the potential of GRACE data assimilation to improve TWS and groundwater estimates. However, the assimilation of TWS does not guarantee accurate estimation of surface SM [Li *et al.*, 2012], and vice versa.

Assimilating multiple observations of the water cycle components should maximize consistency between water balance variables and result in improved water balance estimates. In this study, the feasibility and benefits of jointly assimilating SMOS-derived SM and GRACE-derived TWS estimates into a global water balance model (i.e., the World-Wide Water model (W3) [van Dijk *et al.*, 2013], see section 2.1) was investigated. To assess the performance of the joint assimilation, the open-loop model (without assimilation), the assimilation of SMOS data only, and the assimilation of GRACE data only, respectively, were conducted as comparison against the joint assimilation results. In situ surface SM, root-zone SM, evapotranspiration (ET), streamflow, and groundwater level observations were used to evaluate the assimilation results (section 3). SMOS-observed near-surface SM and GRACE-observed TWSA were also used as independent data sets to evaluate either GRACE-only or SMOS-only assimilation experiment. TWSA estimated through SMOS-only data assimilation were evaluated against GRACE TWSA data to examine the influence of SM assimilation on TWSA estimates. Conversely, SMOS observations were used to evaluate surface SM estimates in the GRACE-only assimilation experiment as ancillary-independent observations in addition to in situ measurements. The deficiencies of the assimilation of either SMOS or GRACE data only and the comparative benefits of joint assimilation for estimating soil moisture profile, groundwater, and fluxes are outlined (section 4).

## 2. Materials and Method

### 2.1. Hydrological Modeling

The hydrological model employed in this study is the World-Wide Water (W3) model [van Dijk *et al.*, 2013] (available at <http://www.wenfo.org/wald/>). It is a global water balance model based on the landscape hydrology component model of the Australia Water Resource Assessment system (AWRA-L) [van Dijk, 2010a; van Dijk and Renzullo, 2011]. Full technical details about AWRA-L can be found in the model technical documentation [van Dijk, 2010a]. The W3 model consists of a grid-based, one-dimensional landscape hydrological model with modules describing surface water and groundwater dynamics and snow. It can be considered as a hybrid between a simplified grid-based land surface model and a “lumped” catchment model of water balance, vegetation ecohydrology, and phenology [van Dijk *et al.*, 2013].

Soil water and energy fluxes are simulated individually for two hydrological response units (HRUs), namely, deep-rooted vegetation and shallow-rooted vegetation. Each of the HRUs occupies a fraction of each grid cell  $f_{HRU}$ . The groundwater and surface water (rivers, lakes, and reservoirs) dynamics are simulated at grid cell level, effectively representing individual catchments. Lateral water distribution between grid cells is not considered in the vertical water balance estimation. Net radiation is the sum of net short-wave radiation and net long-wave radiation [Brutsaert, 1975]. Precipitation is partitioned into interception evaporation and net precipitation. The net precipitation is partitioned into infiltration, infiltration excess surface runoff, and saturation excess runoff [van Dijk, 2010a].

W3-simulated TWS is the integration of soil moisture, groundwater, surface water, snow, and vegetation water storage. The soil water storage is partitioned into individual stores for three layers: top layer  $S_o$ , shallow root layer  $S_s$ , and deep root layer  $S_d$  in equivalent water height. Fluxes for these three unsaturated soil layers comprise infiltration, soil evaporation, drainage, and root water uptake. Layer thickness and porosity are not separately specified to avoid model parameter estimation equifinality issues [Renzullo *et al.*, 2014]. Instead, a maximum water holding capacity  $S_{zFC}$  (field capacity) is specified for each layer  $z$ . Spatial estimates of soil water availability from the Australian Soil Resource Information System (<http://www.asris.csiro.au>) were used to estimate the equivalent physical thickness of the W3-modeled soil layer. Thickness can be estimated by the proportion of field capacity water storage to the available water content (i.e., the difference between field capacity and wilting point for each soil layer). The resulting thicknesses of the top-layer soil in W3 are 5–10 cm. The shallow and deep-root soil layers have an estimated thickness between 15–25 cm and 3–6 m, respectively.

Groundwater balance terms include groundwater storage,  $S_g$ , recharge from deep drainage, capillary rise (estimated with a linear diffusion equation), evaporation from groundwater saturated areas, and discharge into streams (estimated with a linear reservoir model) [Peña-Arancibia *et al.*, 2010; van Dijk, 2010a, 2010b]. The river water balance comprises surface water storage,  $S_r$ , inflows from runoff and discharge, open water evaporation, and catchment water yield [van Dijk, 2010a]. A simple but widely tested snow model used in HBV96 (Hydrologiska Byråns Vattenbalansavdelning model) was implemented in W3 for snow water balance estimation [Bergström *et al.*, 1995]. Finally, it is assumed that 80% of vegetation biomass consists of water.

Global daily gridded  $0.5^\circ$  precipitation, short-wave and long-wave downward radiation, air temperature, wind speed, surface pressure, humidity, and snow rate from the WATCH (Water and Global Change) Forcing Data methodology applied to ERA-Interim (WFDEI) [Weedon *et al.*, 2014] (available at <https://wci.earth2observe.eu/>) were used as meteorological inputs to the model. A global tree cover fraction map [Hansen *et al.*, 2003] was used to determine the vegetation fraction of each HRU. An albedo climatology was derived from Moderate Resolution Imaging Spectrometer white-sky albedo [Moody *et al.*, 2005] (<http://modis-atmos.gsfc.nasa.gov/ALBEDO/>). The parameter values used in this study are based on those from AWRA-L version 0.5 [van Dijk, 2010a].

### 2.2. Satellite Observations

#### 2.2.1. SMOS Soil Moisture Retrieval

SMOS observations allow retrieval of near-surface SM at global scale with a repeat cycle of 2–3 days [Kerr *et al.*, 2001]. The SMOS satellite is in a sun-synchronous orbit that has equatorial overpasses at 6:00 A.M. ascending and 6:00 P.M. descending. The signal depth of the SMOS L-band observations is typically in the range of 0–5 cm, depending on the degree of soil wetness. Daily global SM retrievals from the Level 3

CATDS (Centre Aval de Traitement des Données SMOS) product [Jacquette *et al.*, 2010] from January 2010 to December 2013 were used. The Level 3 SM retrieval algorithm is based on the ESA level 2 processor [Kerr *et al.*, 2012] but enhanced using a multiorbit retrieval method. The retrievals are available for both ascending and descending orbits on a regular 25 km EASE (Equal Area Scalable Earth) grid instead of the irregular ISEA (Icosahedral Snyder Equal Area) system [Kerr *et al.*, 2008]. The data quality index, which considers the error in the retrieval as well as the accuracy of the brightness temperatures, quantifies the uncertainty in the retrievals.

The daily SM estimates used in the assimilation were derived from ascending passes, since the retrievals from early morning or nighttime brightness temperatures show better agreement with in situ measurements [Jackson *et al.*, 2012; Dente *et al.*, 2012; de Jeu, 2003; Draper *et al.*, 2009]. To facilitate assimilation into the W3 model, SMOS SM retrievals were upscaled from their original  $0.25^\circ$  resolution to the W3 modeling grid of  $0.5^\circ$  resolution by simple averaging to be consistent with the forcing data.

### 2.2.2. GRACE Total Water Storage Estimates

Since 2002, GRACE has measured variations in the regional gravity field to provide unique measurements of monthly mass changes at regional to global scale. Changes in water storage induce mass redistribution and, therefore, can be estimated from GRACE after removing atmospheric, ocean, and other time-variable gravity effects. The total water storage (TWS) change estimates used in this study were obtained from the recent release of the monthly  $3^\circ \times 3^\circ$  Jet Propulsion Laboratory (JPL, <http://grace.jpl.nasa.gov>) mascon solution (JPL-RL05M) [Watkins *et al.*, 2015]. The mascon surface mass changes are provided with a spatial sampling of  $0.5^\circ$  resolution due to the boundaries of mascons locating parallels of  $0.5^\circ$  increments. The value of each  $0.5^\circ \times 0.5^\circ$  grid inside a corresponding mascon is identical. JPL-RL05M used surface spherical cap mascons to directly estimate mass variation from the intersatellite range-rate measurements. The regularization used employs a combination of quasi-global geophysical models and altimetry observations to obtain accurate mass flux estimates globally and eliminates the need for empirical destriping filtering. A glacial isostatic adjustment (GIA) correction has been applied based on the model introduced by Geruo *et al.* [2013]. Additional scaling factors derived from hydrological modeling [Landerer and Swenson, 2012] for the interpretation of signals at submascon resolution were not applied to the data in this study. Uncertainty in each mascon derived, following Wahr *et al.* [1998], is provided along with the product. Each monthly TWS estimate represents the surface mass anomaly relative to the baseline average over January 2004 to December 2009. To obtain absolute TWS estimates, the averaged model-simulated TWS over the same period was added to the GRACE TWSA estimates in the assimilation. Twelve years of GRACE TWS change estimates from April 2002 to December 2013 were used in this study.

### 2.3. Data Assimilation Method

In this study, two single-observation assimilation experiments (i.e., the SMOS-only assimilation or GRACE-only assimilation, respectively) were conducted as comparisons to the joint assimilation of SMOS and GRACE observations. SMOS SM retrievals were assimilated into the W3 model using both the EnKF (Ensemble Kalman Filter) and EnKS (Ensemble Kalman Smoother). GRACE TWSA estimates were assimilated into the model using the EnKS with a 1 month assimilation window considering temporal error correlations between each day. Near-daily SMOS SM and monthly GRACE TWSA retrievals were jointly integrated into the W3 model through the EnKS with a 1 month assimilation window to resolve their difference in temporal resolution. Like most data assimilation approaches, our approach explicitly acknowledges that precipitation estimates are uncertain. As a result, water balance is not necessarily maintained, that is, changes in the total water storage in each control volume (i.e., grid cell TWS) may vary from the net sum of fluxes (i.e., the original precipitation estimate, evapotranspiration, and streamflow). This is addressed in section 4.4.

#### 2.3.1. Ensemble Kalman Filter and Ensemble Kalman Smoother

The EnKF is a Monte-Carlo implementation of the Bayesian state update problem that was first introduced by Evensen [1994] to improve the computational feasibility for high-dimensional systems. It is relatively simple and efficient and has become one of the most popular approaches for assimilating satellite data [e.g., Reichle *et al.*, 2002; Crow and Wood, 2003; Clark *et al.*, 2008; Renzullo *et al.*, 2014; Lievens *et al.*, 2015]. The ensemble of model states is generated by propagating the model forward in time with perturbations, known as forecast states. The forecast state ensemble is used to determine model covariances under the assumption of unbiased (i.e., random only) model error. In the analysis or update step, the forecast states

representing the uncertainty in model states are adjusted toward the observations by the Kalman gain matrix, which is determined by model and observation error covariances.

The EnKS is a sequential smoother using only the ensemble of forward-in-time model states and bears a strong resemblance to the EnKF [Evensen and Van Leeuwen, 2000]. Unlike the EnKF, the EnKS computes the analysis from previous time steps up to the current time step within an assimilation window, and information at assimilation time is propagated backward in time using the ensemble covariances. A fixed-lag (or assimilation window) is defined in practical implementations to improve computational efficiency [Cohn et al., 1994]. The assimilation window is determined based on the assumption that the observations will only impact the states in this time interval. The EnKS also eliminates discontinuities or spikes otherwise obtained with sequential filtering of infrequent observations. The benefits of EnKS over EnKF have been demonstrated in several studies [e.g., Evensen and Van Leeuwen, 2000; Dunne and Entekhabi, 2006; Dunne et al., 2007].

Generation of an ensemble with an appropriate spread is a critical step in the ensemble-based assimilation. The ensemble spread should be large enough to allow the observations to influence model estimates [Renzullo et al., 2014]. Inappropriate ensembles will impact on model error covariances and place undue emphasis on either the observations or the modeled forecast, thus affecting the correlated states [Turner et al., 2008]. The initial conditions of the ensembles were perturbed and optimized by a 10 year ensemble open-loop spin-up from 1992 to 2002 to reach dynamic equilibrium. The meteorological forcing data for the model were perturbed to generate an ensemble of forecast states. Each ensemble member  $i$  of the state variable  $x$  at current time step ( $t$ ) can be expressed in a discrete form as

$$x_t^{i-} = f(x_{t-1}^{i+}, u_t^i, \alpha, \omega_t^i) \quad i=1, \dots, M, \tag{1}$$

where  $f$  represents the hydrologic model and  $u$ ,  $\alpha$ , and  $\omega$  indicate the forcing data, model parameters, and model error, respectively. The superscripts “-” and “+” represent the forecast and analysis state, and  $M$  denotes the number of ensemble members. In this study, 100 ensemble members were used to ensure an accurate approximation of the error covariances while maintaining computational efficiency.

A previous assimilation study with the closely related AWRA-L model by Renzullo et al. [2014] found that daily precipitation, incoming short-wave radiation, and average air temperature were the most important forcing variables and that the perturbation of these variables ensures adequate ensemble spread. Therefore, radiation and air temperature were perturbed with an additive error, and precipitation was perturbed with a multiplicative error. Gaussian noise of  $50 \text{ W m}^{-2}$  was added to the short-wave radiation, while air temperature was perturbed with an additive error of 2K. We assumed a multiplicative error in precipitation ( $P_g$ ) by taking a univariate random sample between  $\pm 0.6 P_g$  to avoid negative rainfall for low or zero rainfall values.

The satellite observations available at measurement time  $t$  can be gathered in a vector  $y_t$  with the uncertainties specified in the random error  $\epsilon$  such that

$$y_t = \mathcal{H}(x_t^{i-}) + \epsilon_i, \quad \epsilon \sim N(0, R), \tag{2}$$

where  $\mathcal{H}$  is the observation operator that maps the state vector  $x$  to the observation space. In both EnKF and EnKS, the analysis state for each ensemble member can be updated with the forecast state and a weighted difference between the observation and model prediction as

$$x^{i+} = x^{i-} + P^{-1} H^T (H P^{-1} H^T + R)^{-1} [y - \mathcal{H}(x^{i-}) + \epsilon_i], \quad i=1, \dots, M, \tag{3}$$

where the model error covariance  $P$  can be computed from the ensemble of forecast states. If the model error covariance  $P$  approaches zero, less weight is gained from the observation  $y$ . On the contrary, if the observation error tends toward zero, the analysis states are dominated by the observations.

### 2.3.2. Assimilating SMOS Only

In the EnKF, model forecast error covariance at time  $t$  is computed as

$$P_t^- = \frac{1}{M-1} \sum_{i=1}^M [x_t^{i-} - \bar{x}_t^-] [x_t^{i-} - \bar{x}_t^-]^T, \tag{4}$$

where the analysis state is only influenced by the observation and model error covariance at the update time  $t$ . However, all the forecast states within a smoothing interval are updated together with a set of available observations in the EnKS. Therefore, the temporal correlations within the observation and model forecast states are considered in the error covariance matrices.

Both EnKF and EnKS were employed to assimilate SMOS-derived SM data in the W3 model. The model states  $x$  for update were the W3 simulated top and shallow-layer soil water storage for two HRUs (shallow-rooted and deep-rooted vegetation, i.e.,  $S_{0hru1}$ ,  $S_{0hru2}$ ,  $S_{Shru1}$ ,  $S_{Shru2}$ ). The SMOS observations impact on the model-simulated deeper soil water storage indirectly through the percolation process from the top soil layer and directly through the adjustments from the error correlation structure in the analysis step. The model states of each grid cell were updated independently without considering neighboring grid cells. The analysis increments of two HRUs for each grid cell were calculated separately.

Before the assimilation, SM observations were rescaled to remove systematic difference between the model and observations [Reichle and Koster, 2004; Renzullo et al., 2014; Koster et al., 2009]. This is mainly because the W3 model simulates soil water storage in equivalent water height but SMOS SM retrievals are in volumetric water content. Scaling was done by a mean and variance matching, which ensures the same statistical distribution between model and observations for an effective adjustment of the model estimates. The observations were transformed into model space without modifying the dynamics of the data.

The observation operator  $\mathcal{H}$  was the relative wetness  $\omega$  in this case, due to the inconsistency in units and soil layer thickness between the SMOS observations and W3 model. Relative wetness was calculated as

$$\mathcal{H} = \omega = (1 - f_{sat})\omega_0 + f_{sat}, \quad (5)$$

where  $\omega_0$  is the relative wetness of the unsaturated soil column, derived by scaling the top soil layer water storage by the field capacity (i.e.,  $S_0/S_{0FC}$ ) for each HRU, and  $f_{sat}$  is the fraction of saturated area.

To avoid ensemble collapse and to optimize the use of observations, the covariance inflation technique introduced by Anderson and Anderson [1999] was applied to the top soil layer water storage estimates. Instead of applying a fixed inflation factor all the time, we inflated the ensemble only when the model error was less than 5%. This rational was used to ensure model uncertainties competitive with SMOS uncertainties to allow SMOS to impact on the model states. The inflation factor was calculated dynamically from the variance of the top-layer storage estimates based on error propagation theory. This procedure eliminated the under-estimation of the model error, especially during low or zero rainfall period. Without covariance inflation, error variance would decrease in time to low values, and therefore the observation would not impart constraint on the model estimates [Houtekamer and Mitchell, 2005].

In the EnKF, the states were updated instantaneously when the SMOS observation was available. In the EnKS, by contrast, all of forecast states in a month were entered in one vector and updated jointly on the last day of a month. The temporal and spatial varying observation errors used in the assimilation were derived from the uncertainties of the SM provided along with the SMOS product. Since the observations were transformed to relative wetness instead of absolute values, the uncertainties of the relative wetness derived from SMOS were transformed using the same scaling factor applied to the original SMOS SM data.

### 2.3.3. Assimilating GRACE Only

GRACE TWS change estimates represent the average TWS change over a month. The W3 model, however, simulates TWS at a daily time step. We used the EnKS with a 1 month assimilation window to assimilate GRACE TWS change. The long-term TWS mean from the open-loop model simulation was added to GRACE TWS anomalies to obtain the absolute TWS estimates. The water storage components from the W3 model comprised the system states and were updated individually with GRACE estimates. We used the 3° mascon solutions with a spatial sampling at 0.5° resolution, without considering the spatial correlation between neighboring grids. Thus, there was no variation in TWS anomalies inside the grid cells corresponding to each 3° mascon. GRACE TWS signals were disaggregated vertically into changes in the individual water stores and temporally into daily variations through the assimilation process.

$$\mathcal{H} = \frac{1}{N} \sum_{n=1}^N [f_{HRU1} (S_{0,hru1}^n + S_{S,hru1}^n + S_{d,hru1}^n + S_{snow,hru1}^n + S_{veg,hru1}^n) + f_{HRU2} (S_{0,hru2}^n + S_{S,hru2}^n + S_{d,hru2}^n + S_{snow,hru2}^n + S_{veg,hru2}^n) + S_g^n + S_r^n]. \quad (6)$$

We calculated model predicted monthly averaged TWS using all the daily TWS estimates in a month as the observation operator  $\mathcal{H}$  (equation (6)). Since the water stores associated with the soil (three layers), snow, and vegetation water are simulated independently with two HRUs, and groundwater and surface water are

simulated at the grid scale, all the daily states in a month were gathered in a  $(5 \times 2 + 2) 12N \times 1$  state vector for each ensemble member (i.e., 12 states per day for  $N$  days in a month). The  $N$ -day state error variance and observation state error covariance were computed, and then used to compute the analysis increments for individual daily water stores. In the assimilation, the ensemble of forecast states was established using all daily forecasts in the month. The smoother was applied at the end of the month and updated all states back to the first day of the month through the temporal error correlation. Next, the states of the first day from the next month were initialized with the analysis states of the last day from the previous month. The perturbation of the observations was temporally and spatially independent using the uncertainties provided with the JPL-RLM05 product.

#### 2.3.4. Joint Assimilation

Different from the single-observation assimilation experiments, joint assimilation provides multiple constraints to the W3 model estimates. We applied an EnKS with a 1 month assimilation window to assimilate the SMOS SM and GRACE TWS observations into the W3 model. The state vector was the same as for the GRACE-only experiment, including all daily water storage compartments for a month. The observation vector was established with all available SMOS observations during the month and a single monthly GRACE observation. The observation operator in the joint assimilation combined the operator for the assimilation of SMOS and GRACE data, respectively. The model-predicted daily relative wetness of the top soil layer was calculated as explained in section 2.3.2, while model-predicted TWS was treated identically as the GRACE-only experiment (see section 2.3.3). The analysis increments of the states were calculated from both SMOS and GRACE data based on the error variance and covariance matrices (equation (3)). Therefore, the degree of influence from the observations on the model states is related to the relative error magnitudes of the model and both SMOS and GRACE observations.

The mismatch in dynamic range and observation frequency required special attention. There were 2 orders of magnitude difference between the units of SM and TWS, resulting in large differences in the magnitude of uncertainties (i.e.,  $\sim 0.04 \text{ m}^3/\text{m}^3$  for SM and  $\sim 20 \text{ mm}$  for TWS). The large observation uncertainties of GRACE assigned the corresponding elements a relatively smaller value in the Kalman gain matrix, resulting in less weight given to the GRACE observations. There were about 10 SMOS observations per month and only 1 monthly GRACE observation, thus the analysis increment for each individual state was impacted by 10 SM observations and 1 TWS observations. Left unaddressed, the analysis increments gained from SMOS and GRACE data would therefore be imbalanced, leading SMOS to unduly dominate the model estimates. To account for this unit disparity and to ensure neither observations inappropriately dominated the model estimate, a weighting factor was applied to the observation uncertainties. We conducted several experiments with different scaling factors for the observation uncertainties to allow SMOS and GRACE to have approximately equal weighting in the state vector updating process. Three of those experiments are described here, i.e., assimilation with original observation uncertainties, multiplying SMOS uncertainties by 2 and multiplying GRACE uncertainties by 0.5, respectively.

## 2.4 Model Evaluation

We used GRACE-observed TWS anomalies to validate the TWS estimates updated by the SMOS-only assimilation, and SMOS SM to validate SM estimates updated by assimilation of GRACE only. This analysis was helpful to evaluate the performance of the single-observation assimilation and to investigate whether there was any conflicting information imparted by the two observations. In addition, in situ measurements of near-surface SM, root-zone SM, groundwater level, evapotranspiration, and streamflow were used to validate related model-simulated water balance variables in comparison to the open-loop model simulation. These measurements are described in the following sections.

### 2.4.1. Soil Moisture Observations

Three separate Australian networks of in situ SM sensors were used in the evaluation of our modeling results: OzNet, OzFlux, and CosmOz [Holgate *et al.*, 2016] (Figure 1a). OzFlux and CosmOz sites are spread across Australia, while OzNet provides dense measurements for one catchment (that of the Murrumbidgee River) in southeast Australia. OzFlux is a national ecosystem research network providing observations of energy, carbon, and water exchange between the atmosphere (<http://www.ozflux.org.au>). CosmOz is a network of cosmic ray sensors containing 10 calibrated stations out of 14 total stations across Australia (<http://cosmoz.csiro.au>). OzNet contains 63 monitoring stations in the Murrumbidgee River catchment in New South Wales, Australia [Smith *et al.*, 2012]. Most OzNet and OzFlux stations use Campbell Scientific water

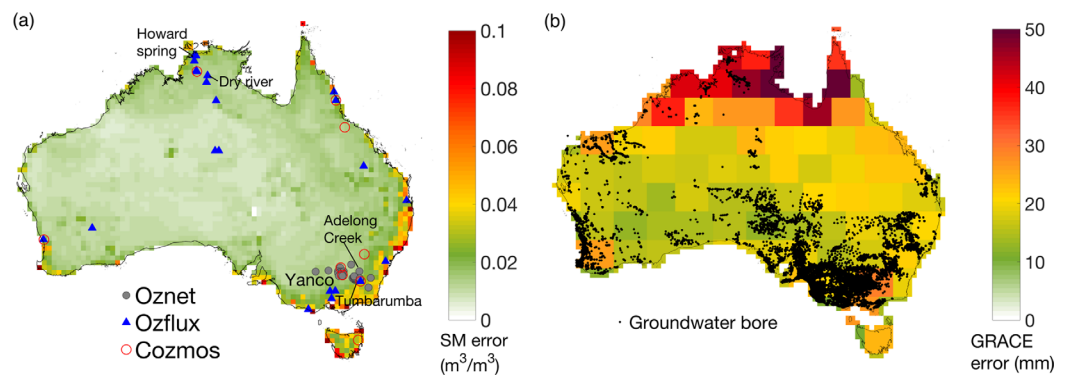


**Figure 1.** In situ observation networks for validation: (a) locations of soil moisture probes from OzNet, OzFlux, and CosmOz with a background of temporally averaged error estimates in SMOS soil moisture retrievals; (b) groundwater bores with a background of temporally averaged error estimates of GRACE mascon TWS change estimates.

content reflectometry probes and provide SM at depths from 0 to up to 90 cm. Unlike the point measurements from other networks, the measurement scale of the CosmOz cosmic ray probes have a signal source area with an approximately 600 m radius, i.e., ~30 ha [Desilets and Zreda, 2013]. The signal depth is influenced by water content itself; from ~10 cm depth in saturated soil to ~50 cm in very dry soil [Franz et al., 2012].

We evaluated model-simulated near-surface SM using all available in situ measurements (OzNet, OzFlux, and CosmOz) at 0–10 cm from 2010 to 2013. The CosmOz measurements were used to evaluate surface SM, due to the depth of CosmOz measurements being generally 6–15 cm in wet soil [Hawdon et al., 2014]. Furthermore, measurements from 37 OzNet probes measurements during our assimilation period were used for evaluation of root-zone SM at 0–30 and 30–90 cm depth. For each OzNet, OzFlux, and CosmOz probe, daily SM were computed by averaging all the measurements within the 24 h. The mean of all measurements within a model grid cell was used if these contained multiple probes (locations are available in Table S1). We provisionally assumed these daily averaged measurement to be representative for the coincident model grid cell. Since the averaged effective depth of CosmOz sites is around 10–15cm, the CosmOz sites were included in the evaluation of top-layer soil moisture. In total, there were in situ data for 39 grid cells to evaluate the top-layer SM estimates and 9 grid cells to evaluate the shallow-layer SM estimates. Correlations between in situ data and model-simulated soil water storage at the same depth were calculated to evaluate the accuracy of the estimation, to circumvent the difference in units between model simulations (mm extractable water) and in situ measurements (soil volume %).

#### 2.4.2. Groundwater Observations

There are around 800,000 groundwater monitoring bores spread unevenly across Australia, providing point-scale groundwater level change over time (Figure 1b). The groundwater level data from the Australian Groundwater Explorer (Bureau of Meteorology, <http://www.bom.gov.au/water/groundwater/explorer>) were collected. We chose bores that had more than 24 observations and at least four consecutive months over the period of January 2002 to December 2013. Water level was reported as either depth to water (DTW, depth below a reference point on the bore), standing water level (SWL, distance from the top of the ground surface to the groundwater), or reduced standing water level (RSWL, groundwater elevation above Australian Height Datum). We calculated groundwater level anomalies from these measurements and aggregated them to 309 values on 0.5° grid cells to enable a comparison to model-estimated groundwater storage anomalies. The mean of all the measurements in a grid cell was assumed to be representative of the grid cell, since GRACE detected the average water change inside its footprint and cannot distinguish the difference between aquifers. The number of bores in each grid cell varies from 1 to > 4000; most grid cells with high bore density were located in south-east Australia. Monthly groundwater level anomalies were computed by averaging all the measurements during a month and compared with model simulations owing to the difference of water level baseline for each bore. Specific yield values were not applied to the water level measurements because we only evaluated correlation between groundwater level anomalies and groundwater storage estimates. This avoids errors from assumed specific yield values to contaminate the comparison.

### 2.4.3. Evapotranspiration Observations

Observations from the OzFlux network (<http://www.ozflux.org.au>) were used to evaluate model estimates of daily evapotranspiration (ET) from January 2010 to December 2011. The coincident model grid cell was compared with observations from 16 flux towers. Observations were converted from latent heat flux measurement, integrated over the 24 h period, into model units of mm per day using the latent heat of vaporization (i.e., 2.45 MJ/kg).

### 2.4.4. Streamflow Observations

Streamflow observations from 780 unregulated catchments across Australia [Zhang *et al.*, 2013] were used in the evaluation of monthly modeled streamflow. Where catchment boundaries overlapped several model cells, corresponding cells were averaged to give representative model estimates. Similarly, where several catchments were within a single model cell, the streamflow data were averaged. The catchment boundaries and their coincident model grid cells are shown in Figure S1. In total, there were 84 aggregated catchments available from January 2010 to December 2011 for use in the evaluation of model-simulated streamflow before and after the assimilation.

## 3. Results

### 3.1. Contributions of SMOS and GRACE Data to Different Water Stores

The analysis increments were calculated as percentages to investigate the contributions to different water stores from SMOS data and GRACE data. Figure 2 shows the averaged analysis increments of March and September from three assimilation experiments: the SMOS-only assimilation (EnKF), GRACE-only assimilation, and joint assimilation, respectively. The analysis increments to the top-layer soil water from SMOS-only assimilation was the largest among the three with around 30% (Figure 2a). GRACE data were less correlated with top-layer soil water storage and led to moderate analysis increments (Figure 2b). This appears to be a result of the high variability of near-surface SM in both time and space and the incongruity between daily precipitation and monthly GRACE TWS change observations. Also, the monthly TWS change provided the information of integrated water storage change over a period and may attenuate or cancel out the small magnitude change of surface soil water through the averaging. However, SMOS and GRACE data imparted opposite water variations in east Australia, where SMOS decreased the soil moisture and GRACE increased the soil moisture. Similar conflicting increments were found for the shallow and deep-layer soil moisture between GRACE and SMOS data. Figure 2c shows the analysis increments from both SMOS and GRACE through joint assimilation. The adjustments of top and shallow-layer soil water storage were dominated by SMOS data, similar to SMOS-only assimilation trends but with a reduced amplitude of change. This is probably because the EnKS smoothed the adjustments over a month instead of providing an instantaneously update.

In the SMOS-only assimilation, groundwater storage was not included in the state vector. The analysis increments of groundwater and TWS were caused by the other updated states and model physics. Therefore, assimilating SMOS data alone can greatly impact other states such as groundwater and TWS. However, the analysis increments for groundwater and TWS from the joint assimilation were similar to the increments from GRACE-only assimilation. The magnitude of increments of the joint assimilation was slightly smaller than the GRACE-only assimilation, owing to the inconsistent increments from SMOS data. Thus, assimilating SMOS or GRACE data alone can lead to different water variations for different water layers. Overall, SMOS mainly contributed to update the top and shallow-layer soil water estimates, while GRACE dominated groundwater and TWS estimates.

### 3.2. Consistency With Satellite Retrievals

The top soil layer relative wetness estimated from open-loop model simulation and different assimilation experiments were compared with SMOS-derived near-surface SM (Figure 3a). GRACE-derived TWS anomalies were compared to model-simulated monthly TWS anomalies with and without the assimilation of satellite observations (Figure 3b). The 0.5° model-simulated TWS anomalies were aggregated over each 3° mascon to compare with GRACE data. It is expected that the assimilation of observations would bring model estimates closer to the observations and 99% of correlations passed the significance test. The averaged correlation of SM from SMOS-only assimilation and SMOS data improved to 0.88 and 0.86 for EnKF-SMOS and EnKS-SMOS, respectively (Table 1). Similarly, the correlation of TWS from GRACE-only assimilation and

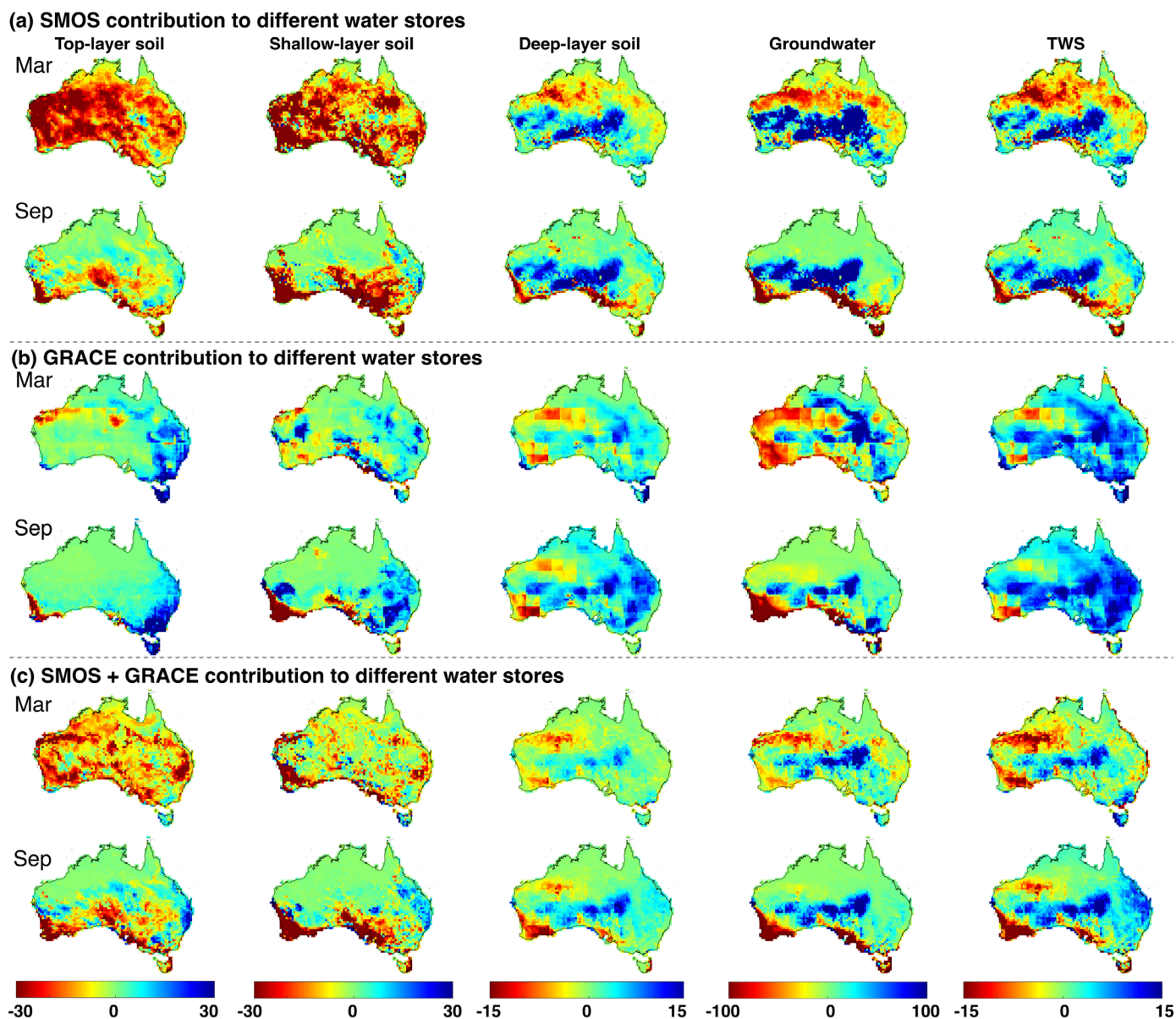


**Figure 2.** Averaged analysis increments to individual water storage components (top, shallow, deep-layer soil water, groundwater storage, and total water storage) in percentage  $(x^2-x^0)/x^0$  in March and September: (a) contributions of SMOS data; (b) contributions of GRACE data; and (c) contributions of the combination of SMOS and GRACE data.

GRACE data improved from 0.57 to 0.75 and the root mean square (RMS) error was reduced by 18 mm on average. This merely demonstrates that the assimilation had the intended effect.

The SM estimates from the GRACE-only assimilation can be compared with SMOS data as an independent evaluation to investigate any potential degradation of GRACE data on surface soil moisture estimation. The results showed that assimilating GRACE data alone overall had no improvement on estimating surface SM and slightly degraded the correlation of SMOS data for more than half of the grid cells (Table 1), compared with the open-loop model simulation. Therefore, assimilating only GRACE data did not produce more accurate estimates of surface soil moisture. On the other hand, assimilating only SMOS data degraded correlation with GRACE TWSA compared to open-loop estimates, with only 30% of the grid cells showing an improved correlation (Table 1). Evidently, assimilation of SMOS data alone also did not improve the estimation of TWS, with a decrease of 0.16 in averaged correlation when the EnKF was used. Therefore, assimilating SMOS data alone can considerably degrade the estimation of TWS.

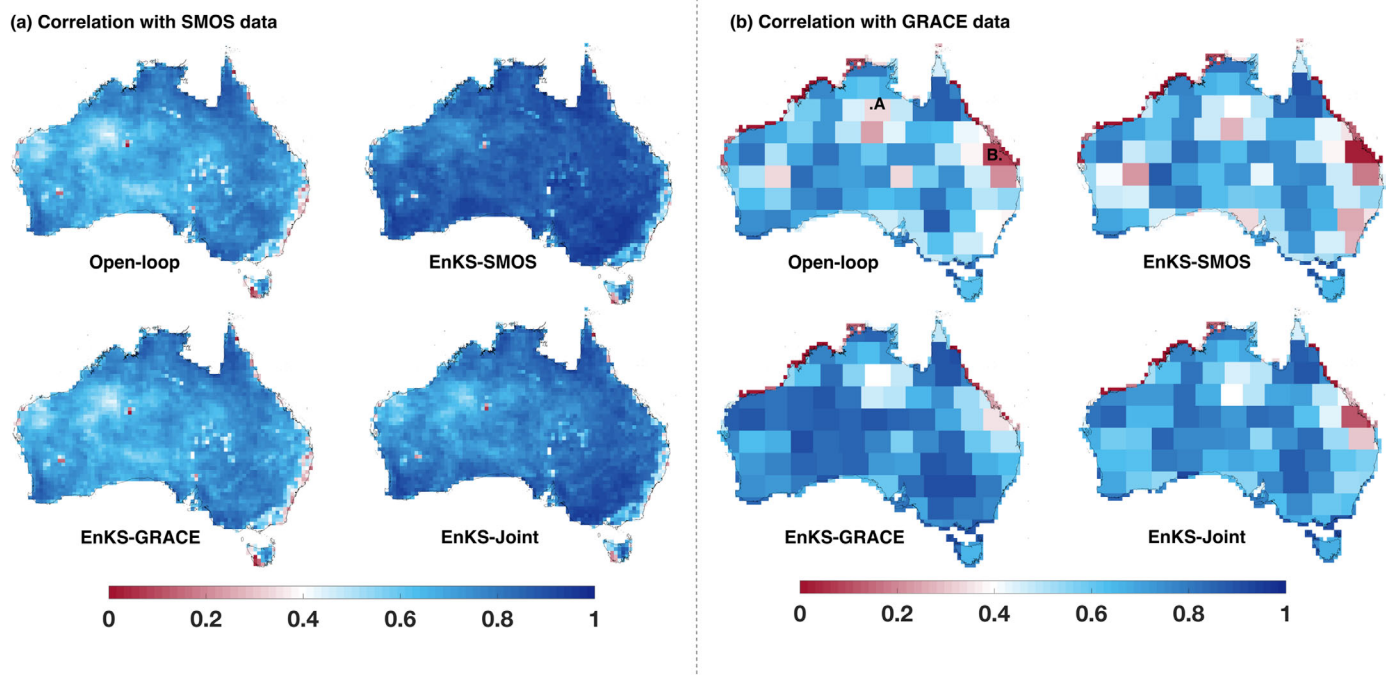


**Figure 3.** Consistency with SMOS and GRACE data: (a) correlations of model-simulated top-layer soil relative wetness with SMOS data; (b) correlations of model-simulated TWS anomalies with GRACE data (open-loop: open-loop model simulation; EnKS-SMOS: assimilation of SMOS only using EnKS; EnKS-GRACE: assimilation of only GRACE using EnKS; EnKS-Joint: joint assimilation. Time series for point A and B are shown in Figure 5).

The joint assimilation achieved similarly good agreement with SMOS data and GRACE data as the SMOS-only assimilation and the GRACE-only assimilation, respectively. Figures 4a and 4b show the time series of the top soil layer relative wetness and TWSA before and after the assimilation at Yanco (located in the south of the Murray-Darling Basin), illustrating the improvement in consistency with SMOS and GRACE data. The joint assimilation sometimes showed less agreement with GRACE data than GRACE-only assimilation, such as Point B in Figure 3b. In other cases, the consistency was improved with the joint assimilation at Point A. The decrease in correlation could be caused by the inconsistent trends between rainfall, SMOS, and GRACE, as shown in Figures 5a–5c. Figures 5e–5h show time series of GRACE, SMOS, rainfall, and model-simulated TWS at Points A and B. The results show that the same trends between rainfall, SMOS, and GRACE can result in improved agreement with GRACE data. However, the agreement degraded at Point B, where GRACE-observed TWS increased but no precipitation and soil moisture increased over time.

### 3.3. Evaluation Against Near-Surface Soil Moisture Measurements

Model-simulated top soil layer relative wetness values were compared with in situ measurements of SM at 5–10 cm depth. Assimilating only SMOS data significantly improved model-estimated near-surface SM

**Table 1.** Spatial-Averaged Correlation of Relative Wetness and TWS With SMOS and GRACE Data for Open-Loop Model Simulation and Different Data Assimilation Experiments Over the Australian Continent<sup>a</sup>

	Open-Loop	EnKF SMOS	EnKS SMOS	EnKS GRACE	Joint ( $\epsilon, \zeta$ )	Joint ( $2\epsilon, \zeta$ )	Joint ( $2\epsilon, 0.5\zeta$ )
Mean $r_{\omega}$	0.69	0.88	0.86	0.69	0.84	0.81	0.8
Mean $rmse_{\omega}$ (%)	0.21	0.12	0.13	0.22	0.14	0.15	0.16
$r_{\omega}^a > r_{\omega}^o$ (%)	NA	94	94	35	94	93	93
Mean $r_{TWS}$	0.57	0.39	0.55	0.75	0.64	0.69	0.76
Mean $rmse_{TWS}$ (cm)	6.80	7.28	6.64	5.04	6.27	5.98	5.47
$r_{TWS}^a > r_{TWS}^o$ (%)	NA	30	46	97	70	85	95

<sup>a</sup> $r_{\omega}$ / $rmse_{\omega}$ : correlation/root mean square error of relative wetness;  $r_{TWS}$ / $rmse_{TWS}$ : correlation/root mean square error of TWS;  $r^a - r^o$ : correlation improvement against open-loop model simulations.  $\epsilon$ : SMOS error;  $\zeta$ : GRACE error.

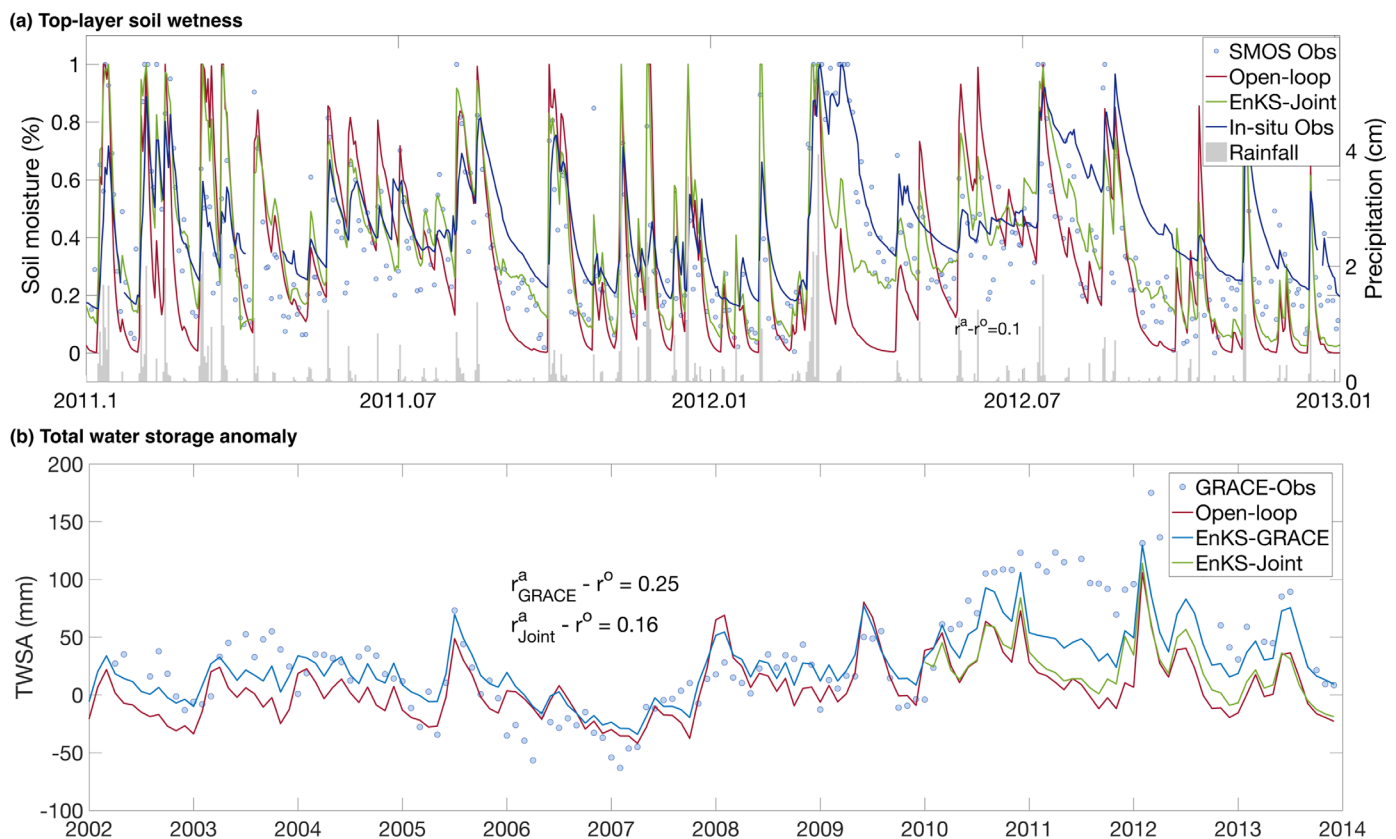


**Figure 4.** Time series of SM and TWSA for Yanco before and after the assimilation: (a) model simulated top-layer soil relative wetness and its consistency with SMOS retrievals, in situ soil moisture measurements and rainfall data; (b) consistency between model-simulated TWS anomalies and GRACE data.

compared to the open-loop estimates, by up to 0.32 in correlation (Figure 6a), but a few sites located close to the water body or in densely vegetated areas showed slightly lower correlations after assimilation. SMOS observations in these locations (e.g., Dry River, Howard Spring, and Tumberumba; Figure 1) showed poor correlation with the in situ measurements. Overall, the EnKS produced slightly better correlations with in situ observations than the EnKF.

The assimilation of only GRACE data did not strongly change the correlation of surface SM with the in situ measurements and was overall not beneficial. Only one grid cell (Adelong Creek; Figure 1) showed better correlation than other assimilation experiments. This may have been the standing water effect on SMOS SM retrieval. Since microwave brightness temperature has a high sensitivity to open water, a small fraction of water bodies within the footprint can result in a considerable overestimation of retrieved SM [Ye *et al.*, 2015]. Joint assimilation generally improved the near-surface SM estimates in most locations, with the same efficiency as the SMOS-only assimilation. The largest improvement was up to 0.27 (Figure 6a and Table S2). Only one grid cell showed a decrease in correlation by 0.1 when compared with the open-loop simulation (CosmOz Tumberumba site located in a wet forest environment, Figure 1).

### 3.4. Evaluation Against Root-Zone Soil Moisture Measurements

Root-zone SM measurements from the OzNet Network at 0–30, 30–90, and 0–90 cm depths were used to evaluate the model-simulated shallow and deep-layer soil water storage estimates. Figures 6b–6d show that assimilating surface SM data from SMOS led to improved soil moisture at different depths, in particular shallow layer soil moisture estimates. An average increase in correlation of 0.15 (Table S3) was found at shallow root zone SM estimates with both EnKF and EnKS. Assimilation of GRACE data only showed more impacts on improving root zone SM than surface SM estimation, with an increase in correlation by up to 0.29 (Figure 6d and Table S3). The joint assimilation combined the information of both surface SM and TWS variation and showed its capability to estimate the shallow-layer soil moisture better than the other three

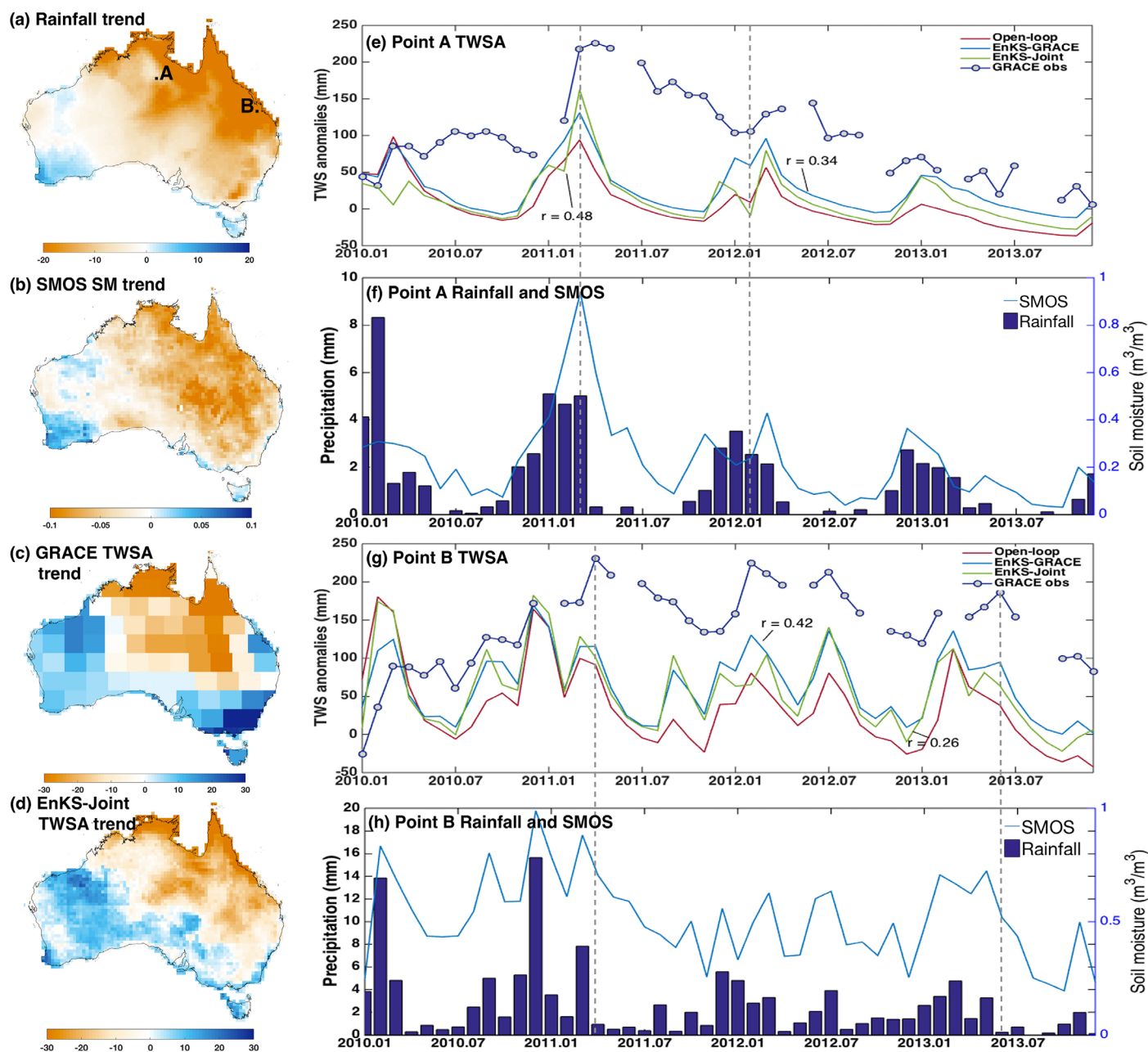


**Figure 5.** Inconsistent trends between rainfall, SMOS and GRACE data over 2010–2013: (a) annual trend of rainfall; (b) annual trend of SMOS-observed soil relative wetness; (c) annual trend of GRACE-observed TWSA; (d) annual trend of model-simulated TWSA through joint assimilation; (e) GRACE-observed TWSA compared with model simulated TWSA at point A; (f) SMOS SM and rainfall observations at Point A; (g) GRACE-observed TWSA compared with model simulated TWSA at point B; (h) SMOS and rainfall observations at Point B.

assimilation experiments. The resulting SM estimates showed an increase of 0.1 in correlation at both shallow and deep layer soil, as well as the full root zone.

### 3.5. Evaluation Against Groundwater Level Measurements

Assimilating only GRACE significantly improved the correlation with groundwater level measurements against model open-loop, as shown in Figure 7a. The correlation is increased by an average 0.1 and up to as much as 0.9 for individual grid cells. Improved agreement between model-estimated groundwater storage change and groundwater level measurements further emphasized the benefit of GRACE TWS assimilation for deeper water stores. Figure 7c illustrates the improvement of the groundwater storage anomalies estimated for the Murray-Darling Basin after assimilation of GRACE data for an extended 12 year period. The magnitude of the groundwater storage changes is intensified due to the assimilation of GRACE data, with

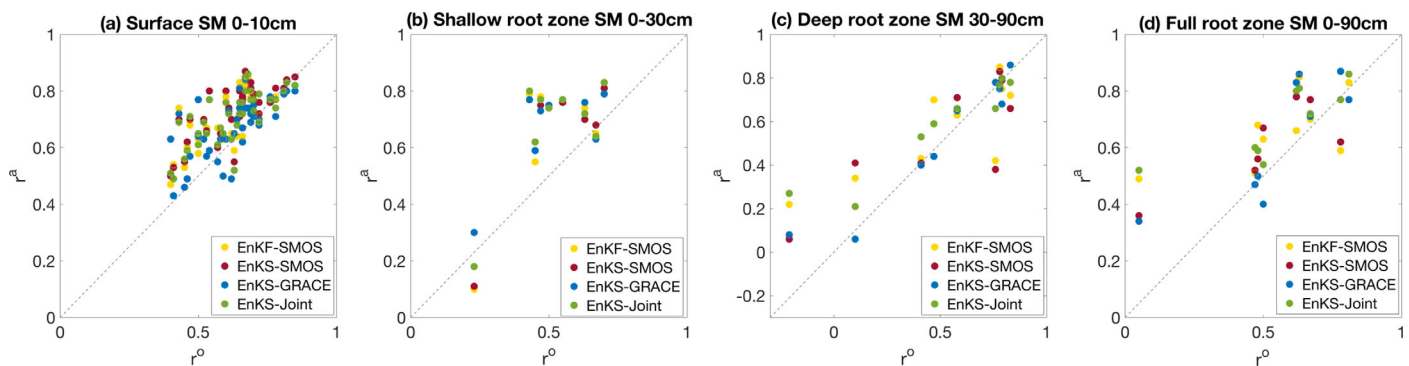


**Figure 6.** Correlation of model-simulated soil moisture with in situ observations ( $r^o$ : correlation of open-loop model simulation;  $r^a$ : correlation after assimilation; yellow dots: the assimilation of SMOS only using EnKF; red dots: the assimilation of SMOS only using EnKS; blue dots: the assimilation of GRACE only; green dots: joint assimilation): (a) correlation of surface soil moisture at 0–10 cm against in situ measurements from OzFlux, OzNet, and CosmOz network; (b) correlation of shallow root zone soil moisture at 0–30 cm against in situ measurements from OzNet; (c) correlation of deep root zone soil moisture at 30–90 cm against in situ measurements from OzNet; (d) correlation of full root zone soil moisture at 0–90 cm against in situ measurements from OzNet.

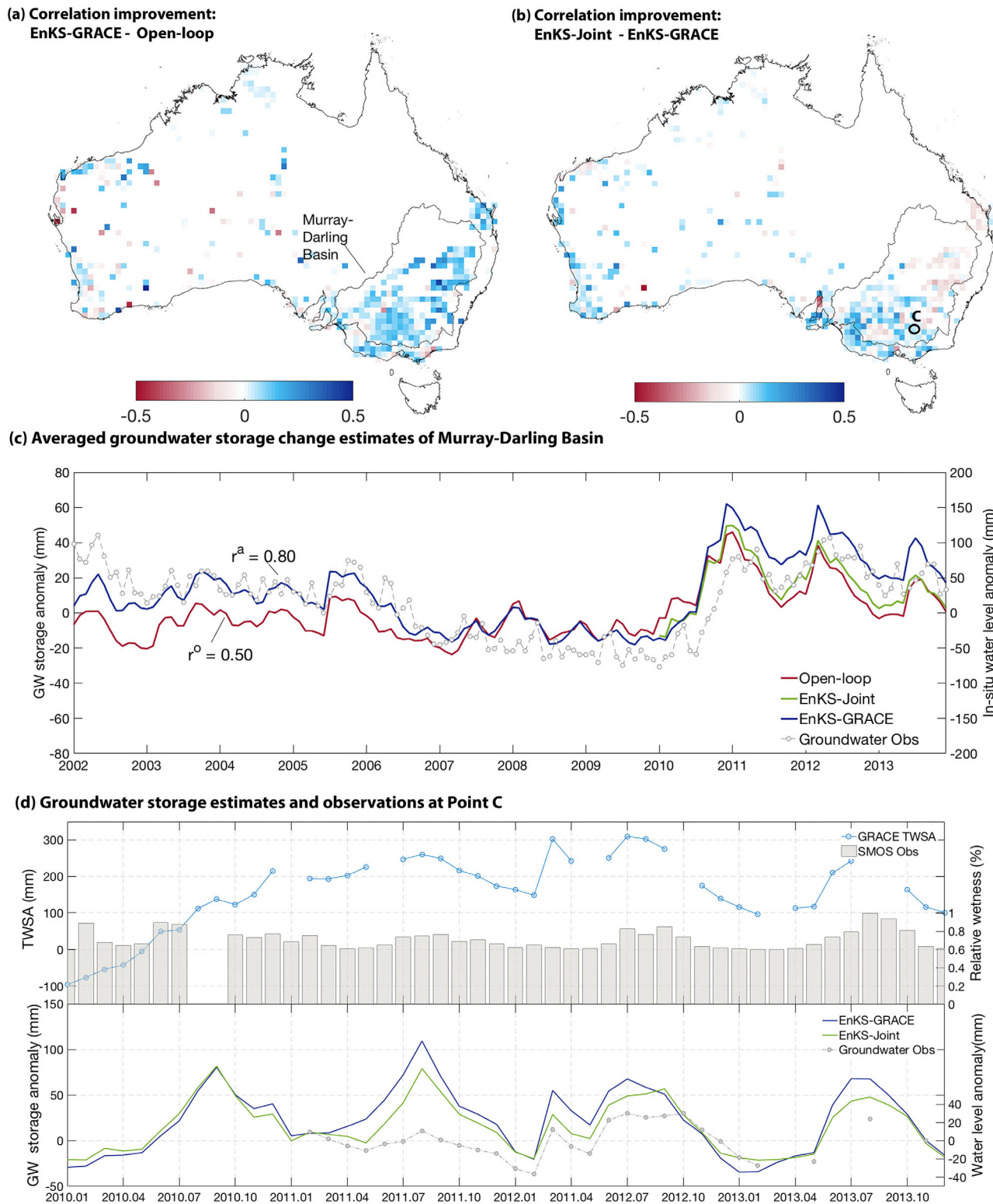
greater depletion in dry periods (2006–2010) and greater increases during wet periods (2010–2013) over the basin. The correlation was improved from 0.50 to 0.80. Note that the actual units vary between the assimilation results and bore data, since specific yield was too uncertain to attempt a conversion from water storage to groundwater level.

Figure 7b shows the locations where the joint assimilation performed better than the GRACE-only assimilation. The majority of grids showed improved correlation than GRACE-only assimilation with an improvement in correlation by up to 0.4. In particular, improved correlation was found in the areas where opposing trends in SMOS SM and GRACE TWS were observed. This indicated the potential to simulate the water loss caused by the groundwater extraction, which is not represented in the model. Figure 7d shows the comparison of simulated groundwater storage change from the GRACE-only assimilation and the joint assimilation at Point C in Figure 7b. This point is located in the agriculture area and has moderate rainfall. However, the relative wetness of soil is over 0.6 at all time (Figure 7d, top). Groundwater bore data showed a decrease in water level during January–April 2011, while GRACE observed no significant change in TWS and the soil moisture increased. The joint assimilation picked up this decrease in groundwater but no decrease was estimated with the assimilation of only GRACE data. Events with a similar decrease occurred in January–April 2012 and July–September 2012, and a larger magnitude of groundwater decrease occurred in the joint assimilation than in the GRACE-only assimilation. Overall, joint assimilation appeared to impart the benefits of the combination of GRACE TWS and SMOS SM as constraints and improved the accuracy of the model-simulated groundwater storage dynamics.

### 3.6. Evaluation of Evapotranspiration and Streamflow

Assimilating SMOS data at daily time step (EnKF-SMOS) showed the biggest impact on improving ET estimates compared to other experiments with an average correlation of 0.83 (Table S4). Conversely, assimilating GRACE data slightly degraded the correlation for most of the points (i.e., 56%). Although the joint assimilation did not significantly improve the ET, the proportion of degradation was reduced compared with other experiments. Assimilating SMOS and GRACE data slightly improved the accuracy of streamflow simulation with average correlation of 0.86 from 0.81 (Table S4). The joint assimilation showed improved correlation for 70% of the grid cells and the correlation increased by up to 0.17 against model open-loop simulation.

In this section, model simulated surface soil moisture, root-zone soil moisture, groundwater, TWS, ET, and streamflow were evaluated with both in situ and satellite observations. Figure 8 summarizes the independent evaluation of individual water balance component. Overall, joint assimilation resulted in more accurate estimation of soil moisture profile at different depths, unlike the assimilation of only one of the two data sets (Figures 8a–8c). Assimilating GRACE data only did not always produce accurate soil moisture estimates and overall less beneficial than either joint or SMOS-only assimilation. Assimilating SMOS SM did not improve the correlation between the model-simulated groundwater storage and the in situ water level measurements. Indeed, the correlation reduced for most of the grid cells compared to the open-loop



**Figure 7.** Correlation increments ( $r^a-r^o$ ) of model-simulated groundwater storage anomalies with in situ water level measurements: (a) the correlation increments of the assimilation of GRACE data alone compared to model open-loop run (blue: improved; red: degraded); (b) correlation increments of the joint assimilation compared to the assimilation of GRACE data alone; (c) time series of averaged groundwater storage simulation of Murray-Darling Basin and in situ water level measurements; (d) improvement of joint assimilation compared with the assimilation of GRACE data alone at Point C (top: GRACE-observed TWSA and SMOS-observed relative wetness; bottom: model-simulated groundwater storage anomalies and in situ water level measurements).

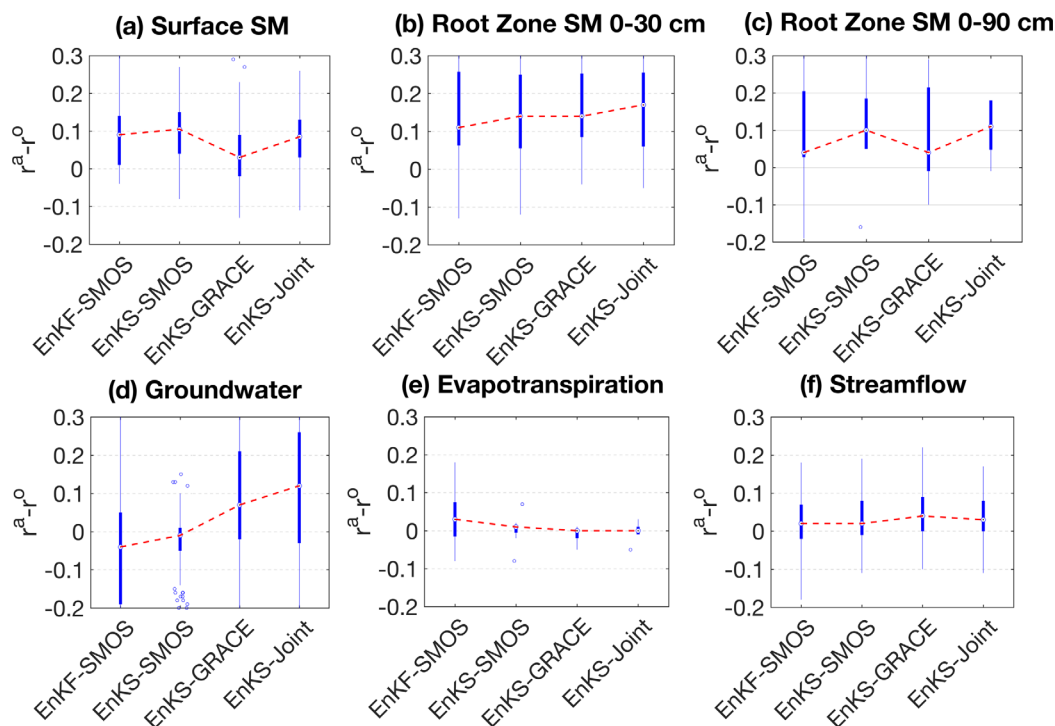


**Figure 8.** Performance of four assimilation experiments on improving different water balance components and statistics of correlation increments (difference between assimilation and open-loop model simulation) (a) surface soil moisture, (b, c) root zone soil moisture at different depths, (d) groundwater, (e) evapotranspiration, and (f) streamflow. The red lines connect the median value of the correlation increments; the blue bars show the interquartile range and the range of correlation increments.

estimates (Figure 8d). The joint assimilation show marginal improvement on ET and streamflow. Notably, though, the joint assimilation had reduced impact on ET and streamflow performance than single-source data assimilation (i.e., reduced proportion of correlation decrease).

#### 4. Discussion

##### 4.1. Disaggregation of Monthly Integrated Water Storage

The objective of the joint assimilation was to combine the information from both SMOS and GRACE data to better estimate the water budget and the variation of its individual component. An important challenge in the assimilation was to allow for the disparity in temporal resolution and spatial resolution at both the vertical and horizontal scales between SMOS data, GRACE data, and model states. In this study, the EnKS-based assimilation framework with a 1 month assimilation window successfully disaggregated the monthly GRACE signals into daily analysis increments for each water store. Unlike the (GRACE-only) data assimilation using a filter-based approach [Eicker et al., 2014; Tangdamrongsub et al., 2015] to update model estimates monthly or update daily estimates by interpolating GRACE data, our EnKS-based assimilation simultaneously updates all daily model states in a month using the monthly GRACE data. Different from the approaches of Zaitchik et al. [2008] and Li et al. [2012] with an even increment for each day, the increments applied over each day of the month were different, thus accounting for temporal error correlations in our method.

The assimilation of GRACE data improved the consistency between model-estimated and GRACE-derived TWS. The clearest improvements were seen in western and southeastern Australia (Figure 3b). The magnitude of TWS change derived from GRACE was larger than modeled estimates. Hence, assimilating GRACE TWS amplified changes in storage and made trends in water loss or gain more distinct (Figure 4b). The joint assimilation of SMOS and GRACE data sometimes led to reduced agreement with GRACE data due to the conflicting constraints. Houborg et al. [2012] also found that the average amplitude of the TWS change from the open-loop model was smaller than the GRACE TWS observations and the adjustments of water

can be subdued by a limited water storage capacity in the model to accommodate the adjustments. The integrated water storage change estimates from GRACE data were partitioned into increments for different water stores through the error correlation structure (Figure 2). In the joint assimilation, the adjustments of soil water stores were dominated by SMOS data, while the contributions to groundwater and TWS were mainly from GRACE data. However, assimilation of SMOS alone can result in considerable changes in TWS. Our study appears to be the first to compare GRACE TWS with TWS estimates after the assimilation of near-surface SM only. The results illustrate that introducing SM observations may lead to improved near-surface and shallow SM estimates, but degraded deeper SM, groundwater, and total TWS estimates. Thus, the relative weighting between SMOS and GRACE data is critical in the joint assimilation. In the experiment of changing the relative weighing between two data sets, we found that model-simulated TWS was sensitive to both SMOS and GRACE data (Table 1). Amplifying SMOS uncertainty and attenuating GRACE uncertainty to accommodate their different dynamic range and observation frequency resulted in a better consistency with GRACE data: the correlation increased from 0.64 to 0.76 and another 25% additional grid cells achieved better correlation than the open-loop simulation. This suggested that SMOS data dominated the original analysis adjustments in the joint assimilation configuration. One likely reason is that the adjustments of TWS came from  $\sim 10$  SMOS observations per month but only one GRACE observation. It also appears that SMOS SM errors may be greater than indicated by the retrieval error estimates. The relative weighting between SMOS and GRACE data needs to be further investigated to optimize their combined use.

In this study,  $3^\circ \times 3^\circ$  GRACE mascon solutions were used, but the TWS and groundwater change can be highly heterogeneous inside each mascon. Figures 5c and 5d compare the annual trend of TWS variation from GRACE and the joint assimilation. The results demonstrated that the joint assimilation produced more detailed spatial variability compared with GRACE mascon data. This is due to the model forward run with high-resolution forcing data and the constraints from SMOS data. The joint assimilation showed good consistency with GRACE data, except for east coast Australia where GRACE uncertainties were relatively large. The joint assimilation also showed better correlation with GRACE TWS in north central Australia compared to the assimilation of only GRACE. This is illustrated in Figures 5e and 5f: the dashed line indicates that SMOS assimilation enhances the analysis by adding or removing more water in the system when SMOS has the same trend in TWS as GRACE. This occurs if the TWS change is mainly due to the soil water variation. Therefore, assimilating SMOS and GRACE together appears to impart more detailed spatial information on the distribution of water, inducing the downscaling of coarse GRACE signals. The TWS estimates with improved spatial resolution from the joint assimilation offers a new tool for monitoring total water storage change with distinct benefits over the original GRACE data.

#### 4.2. Impact on Soil Moisture Profile Estimates

The joint assimilation was able to improve the soil moisture estimation in different layers (Figures 8a–8d). The improved SM correlation at four contrasting depths demonstrates the benefits of joint assimilation on improving the vertical soil moisture profile estimates. In particular, the joint assimilation stood out from the assimilation of only either SMOS or GRACE data in improving root-zone SM estimates. Assimilating SMOS data with EnKF was less robust than EnKS in improving shallow and deep-layer soil moisture. The EnKF corrected the model states instantly as observations became available, while the EnKS updated all previous states back to the first day of the month. The EnKS smoothed water storage estimates over the month, preventing incurring spikes in the updated states and eliminating the impact of noisy observations. Moreover, deeper layer soil water storage or TWS responded slower to precipitation than surface SM, resulting in a time lag with the variation of surface SM. The EnKS with an assimilation window therefore appears more suitable for correcting the states that respond over the course of days or months, such as deep soil water, groundwater, and TWS.

SMOS observations can also provide supplementary information about the water inputs and can mitigate errors in precipitation estimates for areas with sparse monitoring stations. As illustrated in Figure 5a, the positive trend in rainfall evident in north-west Australia was less than observed in both SMOS and GRACE (Figures 5b and 5c), suggesting the error lay in the precipitation data (there are very few rain gauges in this dry and sparsely populated region). An example of comparison between precipitation, in situ measurements and SMOS data at Yanco in Figure 4a showed that the joint assimilation

resulted in a higher more soil moisture prediction during July–October as well as January–April in both 2010 and 2012, consistent with in situ measurements. However, no significant rainfall events were recorded, indicating an error in precipitation estimates or that there was another source inputs water from such as irrigation. Therefore, it appears feasible that the SMOS data can correct errors in the precipitation estimates and detect other source of water inputs, resulting in more accurate estimates of the soil moisture profile. This may have considerable value for agricultural water resource management and drought monitoring.

#### 4.3. Impact on Groundwater Estimates

Similar to Zaitchik *et al.* [2008], Houborg *et al.* [2012], and Tangdamrongsub *et al.* [2015], we found that assimilating GRACE data successfully mitigated the model deficiency in groundwater simulation and led to major improvements in estimating groundwater storage. The correlation with in situ groundwater level measurements was further improved for the majority of grid cells by the joint assimilation, compared to the GRACE-only assimilation. Integrating SMOS data most likely constrained the magnitude of groundwater storage change from TWS changes with more accurate soil water storage estimates. Where they occurred, the opposite trends between GRACE and SMOS provided extra information on the exchanges between soil water and groundwater. This may help quantify groundwater extraction over large areas [Rodell *et al.*, 2009]. In addition, the SMOS data helped to refine the spatial pattern of soil and groundwater storage changes derived from GRACE data. Long *et al.* [2016] found that groundwater depletion estimated from GRACE is likely to be overestimated. They highlighted the importance of incorporating a priori information to refine spatial patterns of GRACE signals. The joint assimilation is less efficient if large water storage changes occur as a result of lateral flow from neighboring cells, e.g., through large rivers or ice mass changes. In such cases, the responsible processes need to be quantified and included [van Dijk *et al.*, 2014]. Overall joint assimilation efficiently improved estimates of groundwater change, potentially resolving the lack of groundwater observations at large scales over much of the world.

#### 4.4. Impact on Evapotranspiration and Streamflow

The joint assimilation framework proposed in this study explicitly acknowledges uncertainty in the model forcing data (e.g. precipitation, temperature, and radiation) and does not conserve mass and energy with respect to the original estimates. While the lack of water balance is not a problem for some applications, there is potential that estimates of other water balance terms may be degraded through data assimilation to compensate for model structural and/or input errors. To investigate this, we evaluated the resulting streamflow and ET with in situ measurements. We found no degradation on both ET and streamflow estimates after the joint assimilation (Table S4 and Figures 8e and 8f). Despite differences in scale, for most locations there was in fact a slight improvement in correlation with ET and streamflow observations and reduced degradation after the joint assimilation as compared to single-observation assimilation experiments (i.e., from 56 to 18% and 31 to 23%, Table S4). The differences of ET and streamflow between assimilation results and open-loop are small, since the fluxes are often reproduced reasonably well in model open-loop with an average correlation of 0.78 and 0.81, respectively (Table S4). The overall marginal improvement may be due to several factors, including a lack of analysis update on water flux terms, weak coupling strength with soil water storage, and “smoothed” variation in the monthly data evaluation.

Evapotranspiration estimates were observed to improve in the EnKF-SMOS experiment with an increase in correlation of up to 0.44 (i.e., from 0.46 to 0.90) compared to open-loop estimates. This is likely because the ET estimates were updated indirectly through updated analysis of soil moisture at daily time step, while they were only adjusted at the beginning of a month with the analysis states at the end of 3 month in the EnKS. Assimilating GRACE data alone had no positive impacts on the estimation of ET with a slight degradation for most of the locations. Tangdamrongsub *et al.* [2015] also found that assimilating GRACE data had no significant impact on streamflow estimation, since monthly GRACE data cannot help to capture the larger peaks of individual streamflow events. To further improve other variables in the water cycle, an approach incorporating the ET, runoff, and precipitation in the adjustment would be considered in future work.

## 5. Conclusions

The accuracy of vertical soil moisture profile, groundwater storage, and total water storage estimates from hydrological modeling was significantly improved through the joint assimilation of satellite-observed near-surface SM from SMOS and TWS from GRACE. The joint assimilation produced more accurate estimates of the key elements of water cycle than the assimilation of only one of the satellite observations, without degradation of streamflow and ET estimates. It improved the performance of GRACE-only assimilation by integrating near-surface water distribution at a finer scale from SMOS, while limiting the degradation of deeper storage estimates caused by the assimilation of SMOS alone.

All of the individual water storage components for different land cover types were updated at daily time steps over a 1 month assimilation window, incorporating the information from both GRACE and SMOS data through temporal error correlations. SMOS provided temporal and spatial varying constraints on near-surface SM and shallow-layer SM estimates from the model. However, assimilating only SMOS SM data degrades the correlation with GRACE TWS data and in situ groundwater level measurements, especially when an EnKF is used. GRACE TWS data mostly contributed to correcting model simulated deep-layer SM and groundwater storage values in the assimilation, also imparting overall constraints on monthly TWS estimates.

Moreover, having constraints on both TWS and near-surface SM can help to mitigate the lack of rain gauges in remote areas and may even help to quantify the impacts of large-scale groundwater extraction. We found that the error in the precipitation data used to force the hydrological model can be corrected through the use of higher resolution SMOS SM observations when both TWS and SMOS show similar increase trends but there was no or low precipitation observed, resulting in more detailed spatial patterns of near-surface soil water variations. The joint assimilation can also detect groundwater loss due to extraction for irrigation purpose, if SMOS shows strong increase in soil wetness but there is no increase in TWS and precipitation.

Integrating SMOS SM and GRACE TWS together successfully combined the strengths of each information source and largely mitigated against their weaknesses. The improved individual water storage estimates offer potential for drought and groundwater monitoring, as well as water cycle reanalysis applications.

### Acknowledgments

The authors thank Nan Ye, Herb McQueen, and Julian Byrne for technical assistance in the data processing. This research was supported under the Australian Research Council's Discovery Projects funding scheme (project number DP140103679). The GRACE land data are obtained from <http://grace.jpl.nasa.gov>, supported by the NASA MEaSUREs Program. The SMOS data were obtained from the "Centre Aval de Traitement des Données SMOS" (CATDS), operated for the "Centre National d'Etudes Spatiales" (CNES, France) by IFREMER (Brest, France). The WATCH-Forcing-Data-ERA-Interim meteorological forcing data set was sourced from [http://www.eu-watch.org/data\\_availability](http://www.eu-watch.org/data_availability), supported by the WATCH project. Calculations were performed on the Terrawulf cluster, a computational facility supported through the AuScope initiative. AuScope Ltd. is funded under the National Collaborative Research Infrastructure Strategy (NCRIS), an Australian Commonwealth Government Program. This research was also undertaken with the assistance of resources from the National Computational Infrastructure (NCI), which is supported by the Australian Government.

### References

- Anderson, J. L., and S. L. Anderson (1999), A Monte Carlo implementation of the nonlinear filtering problem to produce ensemble assimilations and forecasts, *Mon. Weather Rev.*, *127*(12), 2741–2758.
- Andreadis, K. M., and D. P. Lettenmaier (2006), Assimilating remotely sensed snow observations into a macroscale hydrology model, *Adv. Water Resour.*, *29*(6), 872–886.
- Bergström, S., et al. (1995), The HBV model, in *Computer Models of Watershed Hydrology*, edited by V. P. Singh, pp. 443–476, Water Resour. Publ., Highlands Ranch, Colo.
- Brocca, L., F. Melone, T. Moramarco, W. Wagner, V. Naeimi, Z. Bartalis, and S. Hasenauer (2010), Improving runoff prediction through the assimilation of the ASCAT soil moisture product, *Hydrol. Earth Syst. Sci.*, *14*(10), 1881–1893.
- Brutsaert, W. (1975), On a derivable formula for long-wave radiation from clear skies, *Water Resour. Res.*, *11*(5), 742–744.
- Clark, M. P., D. E. Rupp, R. A. Woods, X. Zheng, R. P. Ibbitt, A. G. Slater, J. Schmidt, and M. J. Uddstrom (2008), Hydrological data assimilation with the ensemble Kalman filter: Use of streamflow observations to update states in a distributed hydrological model, *Adv. Water Resour.*, *31*(10), 1309–1324.
- Cohn, S. E., N. Sivakumaran, and R. Todling (1994), A fixed-lag kalman smoother for retrospective data assimilation, *Mon. Weather Rev.*, *122*(12), 2838–2867.
- Crow, W. T., and E. F. Wood (2003), The assimilation of remotely sensed soil brightness temperature imagery into a land surface model using ensemble Kalman filtering: A case study based on ESTAR measurements during SGP97, *Adv. Water Resour.*, *26*(2), 137–149.
- de Jeu, R. A. (2003), Retrieval of land surface parameters using passive microwave remote sensing, PhD thesis, Vrije Universiteit Amsterdam, Amsterdam.
- Dente, L., Z. Su, and J. Wen (2012), Validation of SMOS soil moisture products over the maqu and twente regions, *Sensors*, *12*(8), 9965–9986.
- Desilets, D., and M. Zreda (2013), Footprint diameter for a cosmic-ray soil moisture probe: Theory and Monte Carlo simulations, *Water Resour. Res.*, *49*, 3566–3575, doi:10.1002/wrcr.20187.
- Draper, C., J.-F. Mahfouf, J.-C. Calvet, E. Martin, and W. Wagner (2011), Assimilation of ASCAT near-surface soil moisture into the SIM hydrological model over France, *Hydrol. Earth Syst. Sci.*, *15*(12), 3829–3841.
- Draper, C. S., J. P. Walker, P. J. Steinle, R. A. de Jeu, and T. R. Holmes (2009), An evaluation of AMSR-E derived soil moisture over Australia, *Remote Sens. Environ.*, *113*(4), 703–710.
- Dumedah, G., J. P. Walker, and O. Merlin (2015), Root-zone soil moisture estimation from assimilation of downscaled soil moisture and ocean salinity data, *Adv. Water Resour.*, *84*, 14–22.
- Dunne, S., and D. Entekhabi (2006), Land surface state and flux estimation using the ensemble Kalman smoother during the southern great plains 1997 field experiment, *Water Resour. Res.*, *42*, W01407, doi:10.1029/2005WR004334.
- Dunne, S. C., D. Entekhabi, and E. G. Njoku (2007), Impact of multiresolution active and passive microwave measurements on soil moisture estimation using the ensemble Kalman smoother, *IEEE Trans. Geosci. Remote Sens.*, *45*(4), 1016–1028.

- Eicker, A., M. Schumacher, J. Kusche, P. Döll, and H. M. Schmied (2014), Calibration/data assimilation approach for integrating grace data into the watergap global hydrology model (WGHM) using an ensemble Kalman filter: First results, *Surveys Geophys.*, 35(6), 1285–1309, doi:10.1007/s10712-014-9309-8.
- Evensen, G. (1994), Sequential data assimilation with a nonlinear quasi-geostrophic model using Monte Carlo methods to forecast error statistics, *J. Geophys. Res.*, 99(C5), 10,143–10,162.
- Evensen, G., and P. J. Van Leeuwen (2000), An ensemble Kalman smoother for nonlinear dynamics, *Mon. Weather Rev.*, 128(6), 1852–1867.
- Forman, B. A., R. Reichle, and M. Rodell (2012), Assimilation of terrestrial water storage from grace in a snow-dominated basin, *Water Resour. Res.*, 48, W01507, doi:10.1029/2011WR011239.
- Franz, T. E., M. Zreda, T. Ferre, R. Rosolem, C. Zweck, S. Stillman, X. Zeng, and W. Shuttleworth (2012), Measurement depth of the cosmic ray soil moisture probe affected by hydrogen from various sources, *Water Resour. Res.*, 48, W08515, doi:10.1029/2012WR011871.
- Geruo, A., J. Wahr, and S. Zhong (2013), Computations of the viscoelastic response of a 3-D compressible earth to surface loading: an application to glacial isostatic adjustment in Antarctica and Canada, *Geophys. J. Int.*, 192(2), 557–572.
- Hansen, M., R. DeFries, J. Townshend, M. Carroll, C. Dimiceli, and R. Sohlberg (2003), Global percent tree cover at a spatial resolution of 500 meters: First results of the MODIS vegetation continuous fields algorithm, *Earth Interact.*, 7(10), 1–15.
- Hawdon, A., D. McJannet, and J. Wallace (2014), Calibration and correction procedures for cosmic-ray neutron soil moisture probes located across Australia, *Water Resour. Res.*, 50, 5029–5043, doi:10.1002/2013WR015138.
- Holgate, C., et al. (2016), Comparison of remotely sensed and modelled soil moisture data sets across Australia, *Remote Sens. Environ.*, 186, 479–500.
- Houborg, R., M. Rodell, B. Li, R. Reichle, and B. F. Zaitchik (2012), Drought indicators based on model-assimilated gravity recovery and climate experiment (grace) terrestrial water storage observations, *Water Resources Research*, 48, W07525, doi:10.1029/2011WR011291.
- Houtekamer, P. L., and H. L. Mitchell (2005), Ensemble Kalman filtering, *Q. J. R. Meteorol. Soc.*, 131(613), 3269–3289.
- Huffman, G. J., D. T. Bolvin, E. J. Nelkin, D. B. Wolff, R. F. Adler, G. Gu, Y. Hong, K. P. Bowman, and E. F. Stocker (2007), The TRMM multisatellite precipitation analysis (TMPA): Quasi-global, multiyear, combined-sensor precipitation estimates at fine scales, *J. Hydrometeorol.*, 8(1), 38–55.
- Jackson, T. J., et al. (2012), Validation of soil moisture and ocean salinity (SMOS) soil moisture over watershed networks in the U.S., *IEEE Trans. Geosci. Remote Sens.*, 50(5), 1530–1543.
- Jacquette, E., A. Al Bitar, A. Mialon, Y. Kerr, A. Quesney, F. Cabot, and P. Richaume (2010), SMOS CATDS level 3 global products over land, *Proc. SPIE7824, Rem. Sens. for Agriculture, Ecosystems, and Hydrology XII*, 78240K.
- Joyce, R. J., J. E. Janowiak, P. A. Arkin, and P. Xie (2004), CMORPH: A method that produces global precipitation estimates from passive microwave and infrared data at high spatial and temporal resolution, *J. Hydrometeorol.*, 5(3), 487–503.
- Kerr, Y., J. Vergely, P. Waldteufel, P. Richaume, E. Anterrieu, and R. Moreno (2008), CATDS SMOS L3 processor: Algorithm theoretical baseline document for the soil moisture retrieval (ATBD), *Rep. CATDS-ATBD-SM-L3*, CNES-CESBIO, Toulouse, France.
- Kerr, Y. H., P. Waldteufel, J.-P. Wigneron, J.-M. Martinuzzi, J. Font, and M. Berger (2001), Soil moisture retrieval from space: The soil moisture and ocean salinity (SMOS) mission, *IEEE Trans. Geosci. Remote Sens.*, 39(8), 1729–1735.
- Kerr, Y. H., et al. (2012), The SMOS soil moisture retrieval algorithm, *IEEE Trans. Geosci. Remote Sens.*, 50(5), 1384–1403.
- Koster, R. D., Z. Guo, R. Yang, P. A. Dirmeyer, K. Mitchell, and M. J. Puma (2009), On the nature of soil moisture in land surface models, *J. Clim.*, 22(16), 4322–4335.
- Landerer, F., and S. Swenson (2012), Accuracy of scaled grace terrestrial water storage estimates, *Water Resour. Res.*, 48, W04531, doi:10.1029/2011WR011453.
- Li, B., M. Rodell, B. F. Zaitchik, R. H. Reichle, R. D. Koster, and T. M. van Dam (2012), Assimilation of grace terrestrial water storage into a land surface model: Evaluation and potential value for drought monitoring in western and central Europe, *J. Hydrol.*, 446, 103–115.
- Lievens, H., et al. (2015), SMOS soil moisture assimilation for improved hydrologic simulation in the Murray darling basin, Australia, *Remote Sens. Environ.*, 168, 146–162.
- Long, D., X. Chen, B. R. Scanlon, Y. Wada, Y. Hong, V. P. Singh, Y. Chen, C. Wang, Z. Han, and W. Yang (2016), Have grace satellites overestimated groundwater depletion in the northwest India aquifer?, *Sci. Rep.*, 6, Article 24398.
- Martens, B., D. Miralles, H. Lievens, D. Fernández-Prieto, and N. Verhoest (2015), Improving terrestrial evaporation estimates over continental Australia through assimilation of SMOS soil moisture, *Int. J. Appl. Earth Observ. Geoinf.*, 48, 146–162.
- Moody, E. G., M. D. King, S. Platnick, C. B. Schaaf, and F. Gao (2005), Spatially complete global spectral surface albedos: Value-added datasets derived from terra MODIS land products, *IEEE Trans. Geosci. Remote Sens.*, 43(1), 144–158.
- Peña-Arancibia, J., A. Van Dijk, M. Mulligan, and L. A. Bruijnzeel (2010), The role of climatic and terrain attributes in estimating baseflow recession in tropical catchments, *Hydrol. Earth Syst. Sci.*, 14(11), 2193–2205.
- Reichle, R. H., and R. D. Koster (2004), Bias reduction in short records of satellite soil moisture, *Geophys. Res. Lett.*, 31, L19501, doi:10.1029/2004GL020938.
- Reichle, R. H., and R. D. Koster (2005), Global assimilation of satellite surface soil moisture retrievals into the NASA catchment land surface model, *Geophys. Res. Lett.*, 32, L02404, doi:10.1029/2004GL021700.
- Reichle, R. H., D. B. McLaughlin, and D. Entekhabi (2002), Hydrologic data assimilation with the ensemble Kalman filter, *Mon. Weather Rev.*, 130(1), 103–114.
- Renzullo, L. J., A. I. J. M. van Dijk, J. M. Perraud, D. Collins, B. Henderson, H. Jin, A. B. Smith, and D. L. McJannet (2014), Continental satellite soil moisture data assimilation improves root-zone moisture analysis for water resources assessment, *J. Hydrol.*, 519, 2747–2762, doi:10.1016/j.jhydrol.2014.08.008.
- Rodell, M., and P. Houser (2004), Updating a land surface model with MODIS-derived snow cover, *J. Hydrometeorol.*, 5(6), 1064–1075.
- Rodell, M., I. Velicogna, and J. S. Famiglietti (2009), Satellite-based estimates of groundwater depletion in India, *Nature*, 460(7258), 999–1002.
- Schumacher, M., J. Kusche, and P. Döll (2016), A systematic impact assessment of GRACE error correlation on data assimilation in hydrological models, *J. Geod.*, 90, 537–559.
- Smith, A., J. Walker, A. Western, R. Young, K. Ellett, R. Pipunic, R. Grayson, L. Siriwardena, F. Chiew, and H. Richter (2012), The Murrumbidgee soil moisture monitoring network data set, *Water Resour. Res.*, 48, W07701, doi:10.1029/2012WR011976.
- Sun, C., J. P. Walker, and P. R. Houser (2004), A methodology for snow data assimilation in a land surface model, *J. Geophys. Res.*, 109, D08108, doi:10.1029/2003JD003765.
- Tangdamrongsub, N., S. C. Steele-Dunne, B. C. Gunter, P. G. Ditmar, and A. H. Weerts (2015), Data assimilation of grace terrestrial water storage estimates into a regional hydrological model of the rhine river basin, *Hydrol. Earth Syst. Sci.*, 19(4), 2079–2100, doi:10.5194/hess-19-2079-2015.

- Tapley, B. D., S. Bettadpur, M. Watkins, and C. Reigber (2004), The gravity recovery and climate experiment: Mission overview and early results, *Geophys. Res. Lett.*, *31*, L09607, doi:10.1029/2004GL019920.
- Turner, M., J. Walker, and P. Oke (2008), Ensemble member generation for sequential data assimilation, *Remote Sens. Environ.*, *112*(4), 1421–1433, doi:10.1016/j.rse.2007.02.042.
- van Dijk, A. (2010a), Landscape model (version 0.5) technical description, *AWRA Tech. Rep. 3*, WIRADA/CSIRO Water for a Healthy Country Flagship, Canberra.
- van Dijk, A. (2010b), Climate and terrain factors explaining streamflow response and recession in Australian catchments, *Hydrol. Earth Syst. Sci.*, *14*(1), 159–169.
- van Dijk, A., and L. Renzullo (2011), Water resource monitoring systems and the role of satellite observations, *Hydrol. Earth Syst. Sci.*, *15*(1), 39–55.
- van Dijk, A. I. J. M., J. L. Peña-Arancibia, E. F. Wood, J. Sheffield, and H. E. Beck (2013), Global analysis of seasonal streamflow predictability using an ensemble prediction system and observations from 6192 small catchments worldwide, *Water Resour. Res.*, *49*, 2729–2746, doi:10.1002/wrcr.20251.
- van Dijk, A. I. J. M., L. J. Renzullo, Y. Wada, and P. Tregoning (2014), A global water cycle reanalysis (2003–2012) merging satellite gravimetry and altimetry observations with a hydrological multi-model ensemble, *Hydrol. Earth Syst. Sci.*, *18*(8), 2955–2973.
- Wahr, J., M. Molenaar, and F. Bryan (1998), Time variability of the earth's gravity field: Hydrological and oceanic effects and their possible detection using grace, *J. Geophys. Res.*, *103*(B12), 30,205–30,229, doi:10.1029/98JB02844.
- Walker, J. P., and P. R. Houser (2001), A methodology for initializing soil moisture in a global climate model: Assimilation of near-surface soil moisture observations, *J. Geophys. Res.*, *106*(D11), 11,761–11,774, doi:10.1029/2001JD900149.
- Walker, J. P., G. R. Willgoose, and J. D. Kalma (2001), One-dimensional soil moisture profile retrieval by assimilation of near-surface observations: A comparison of retrieval algorithms, *Adv. Water Resour.*, *24*(6), 631–650.
- Watkins, M. M., D. N. Wiese, D.-N. Yuan, C. Boening, and F. W. Landerer (2015), Improved methods for observing earth's time variable mass distribution with grace using spherical cap mascons, *J. Geophys. Res. Solid Earth*, *120*, 2648–2671, doi:10.1002/2014JB011547.
- Weedon, G. P., G. Balsamo, N. Bellouin, S. Gomes, M. J. Best, and P. Viterbo (2014), The WFDEI meteorological forcing data set: Watch forcing data methodology applied to era-interim reanalysis data, *Water Resour. Res.*, *50*, 7505–7514, doi:10.1002/2014WR015638.
- Ye, N., J. Walker, J. Guerschman, D. Ryu, and R. Gurney (2015), Standing water effect on soil moisture retrieval from l-band passive microwave observations, *Remote Sens. Environ.*, *169*, 232–242.
- Zaitchik, B. F., M. Rodell, and R. H. Reichle (2008), Assimilation of grace terrestrial water storage data into a land surface model: Results for the Mississippi river basin, *J. Hydrometeorol.*, *9*(3), 535–548, doi:10.1175/2007jhm951.1.
- Zhang, Y., N. Viney, A. Frost, A. Oke, M. Brooks, Y. Chen, and N. Campbell (2013), Collation of Australian modeller's streamflow dataset for 780 unregulated Australian catchments, 115 pp., Catchment Manage., Water for a Healthy Country Natl. Res. Flagship.